

## Study Nonlinear Optical Properties Of Two Molecular Forms Of Rhodamine B dye Solution

Shaymaa Jabbar Abdulrazzaq<sup>1,A\*</sup>, Abdulazeez O. Mousa<sup>2,B</sup>, Talib M. Abbas<sup>3,C</sup>

<sup>1</sup>Physics Department, College of Science, University of Babylon, Iraq

<sup>2</sup>Physics Department, College of Science, University of Babylon, Iraq

<sup>3</sup>Physics Department, College of Education for Pure Sciences, University of Babylon, Iraq

<sup>a</sup>[stud.shaymaa.jabbar@uobabylon.edu.iq](mailto:stud.shaymaa.jabbar@uobabylon.edu.iq), <sup>b</sup>[sci.abdul.azeez@uobabylon.edu.iq](mailto:sci.abdul.azeez@uobabylon.edu.iq), <sup>c</sup>[Pure.talib.mohsen@uobabylon.edu.iq](mailto:Pure.talib.mohsen@uobabylon.edu.iq)

---

**Abstract:** In this study two forms of prepared Rhodamine B (RhB) dye at concentration ( $10^{-5}$ ) M in a solvent methanol at room temperature, were measured using a UV-Visible spectrophotometer to determine the linear index of refraction and the linear coefficient of absorption. The results show that the index of refraction increased when acids were added, but decreased when bases were added. The nonlinear optical properties of the samples, such as the nonlinear index of refraction and the nonlinear coefficient of absorbance, were calculated by using two sections of the Z-Scan technique. The first was a closed aperture that was mounted ahead of the detector to determine the nonlinear refractive index. The aperture ahead of the detector was removed (open aperture) to measure the coefficient of nonlinear absorption in the second part. The two cases were carried out with a continuous wave (CW) diode laser with a wavelength of 457 nm and an input power of 112 mW. The results show that two molecular forms of the RhB dye solution a negative refractive index ( $-n_2$ ), which led to self-defocusing and two-photon absorption for an open aperture Z-Scan, indicating that the laser dye in this study can be used in nonlinear optics and optical limiter applications.

**Keywords:** Nonlinear Optical Properties, Rhodamine B, cationic, zwitterion

---

### Introduction

Nonlinear optical organic materials have been studied extensively in the hunt for materials substantial and fast optical nonlinearities. Organic materials with significant third-order nonlinearities can have a refractive index that is intensity dependent and shows nonlinear transmission. Such materials have the potential to be useful in a variety of photonic applications [1].

Intensity-dependent contributions to the refractive index can be caused by a variety of physical causes. A strong light field in a liquid can cause anisotropic molecules to orient, causing the medium to become

anisotropic and the average refractive index to change. Nonlinearity in liquids that contain isotropic molecules may be the result of molecular redistribution or electronic pinning [2].

The xanthene family of dye compounds are generally utilized in dye lasers to produce tunable lasers, and there is much interest in learning more about them. RhB is affected by a variety of parameters, including solvents, concentration, and pH value. The carboxyl group is involved in a classic acid–base equilibrium, in which the acid and basic forms are brightly colored. Due to its high fluorescence quantum yield, it is often utilized as an active medium in tunable lasers [3].

Linear absorption, saturation of absorption (SA) and reverse saturable absorption (RSA) are the three primary absorption processes in dyes [4]. The wavelength, intensity, and excited-state duration are all important factors in absorption. [21-41] The xanthene family includes the RhB dye which is one of the most commonly used dyes in various spectroscopic studies. Our basic aim in the present study is to examine the nonlinear absorption behavior of in the visible region. To our knowledge, this is the first time that the data of nonlinear absorption in RhB dye at 457 nm in methanol solvents containing two acids and two bases, using the usual Z-Scan approach has been published [5].

### Theoretical part

The Z-Scan method is based on a material's intensity-dependent absorption coefficient ( $\alpha$ ) and refractive index ( $n$ ). The following relationships are typically used to characterize them [6,7]:

$$\alpha(I) = \alpha_0 + \beta I \quad (1)$$

$$n(I) = n_0 + n_2 I \quad (2)$$

The linear absorption coefficient is  $\alpha_0$ , the linear refractive index is  $n_0$  and the laser beam intensity is  $I$ . The formula  $|\Delta n| = n_2 I_0$ , where  $I_0$  is the incident laser beam intensity [6], relates the change in refractive index to  $n_2$ . Using the relation, the nonlinear absorption coefficient ( $\beta$ ) can be estimated from open-aperture Z-Scan data. [8,9]:

$$\beta = \frac{2\sqrt{2}}{I_0 L_{\text{eff}}} \Delta T \quad (3)$$

Where  $\Delta T$  is the difference in normalized transmittance between the curve peak at the focal point ( $Z=0$ ) and the base line, and  $L_{\text{eff}}$  is the sample's effective length (thickness) and is given by:

$$L_{\text{eff}} = (1 - \exp(-\alpha_0 L)) / \alpha_0$$

$$(4) \quad (4)$$

Where L is the actual sample length.

The difference between the normalized peak and valley transmittance is  $\Delta T_{P-V} = T_P - T_V$ . The relation is used to compute the variation of  $\Delta T_{P-V}$  as a function of the on-axis nonlinear phase shift at the focus  $|\Delta \phi_0|$  is calculated using the relation [10,11]:

$$\Delta T_{P-V} = 0.406(1-S)^{0.25}|\Delta \phi_0| \quad (5)$$

Where S is the aperture linear transmittance and is given by:

$$S = 1 - \exp(-2r_a^2/\omega_a^2) \quad (6)$$

Where  $r_a$  is the aperture radius and  $\omega_a$  is the beam radius at the entrance of the aperture. The nonlinear refractive index ( $n_2$ ) is calculated from the relation:

$$n_2 = \frac{\Delta \phi_0 \lambda}{2\pi I_0 L_{\text{eff}}} \quad (7)$$

### Materials used

Many studies have focused on the xanthene family, of which RhB dye is a member, due to their higher gain and differences in many aspects (e.g., different solvents and different concentrations). The RhB dye's ( $C_{28}H_{31}N_2O_3$ ) molecular weight is 479.02 g/M [12].

### Solutions preparation

In a number of (250 ml) glass bottles containing (100 ml), a mass of (0.000099 mol) RhB dye was added. The mixture was agitated with a magnetic stirrer at room temperature to obtain a homogenous solution. Organic dye solutions of concentration ( $10^{-5}$ ) M in a methanol solvent were produced. The powder was weighed using a four-digit sensitivity electronic balance (BL 210 S, Germany). The concentration was calculated using the equation below [14].

$$W = \frac{M_w \times V \times C}{1000} \quad (8)$$

Where  $W$  denotes weight of the dissolved material(g),  $M_w$  denotes molecular weight of the material(g/mol),  $V$  denotes volume of the solvent(mL) and  $C$  denotes the concentration(M).

### Effect of solution pH and ionic strength on dye

The number of drops was insufficient as a measure, for the volume of additive had a significant impact on the laser output power and efficiency. As a result, the pH value was chosen as a parameter due to its ease of change and great reproducibility.

The cationic form of RhB dye solutions was generated by adding trace of HCl (37 percent M) to (18 mol) of dye solution once, and another time by adding 18 drops of  $\text{CH}_3\text{COOH}$  (99 percent M) to (18 mol) of dye solution. To produce the zwitterionic form, a drop of NaOH (25-30 percent M) was added to (18 mol) of dye solution, followed by 15 drops of  $\text{NH}_3$  (20 percent M) for adjustments across the range (pH=10). To obtain a homogenous solution, a mixing magnetic stirrer at room temperature was used. Fig.1 shows the chemical structure of the two types of RhB dye [13].

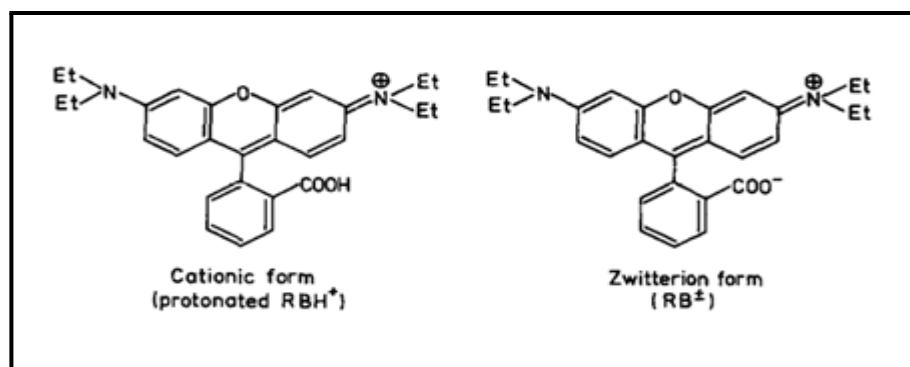


**Fig.1 : Molecular form of Rhodamine B dye [13].**

### UV-Visible spectrophotometer

Shimadzu offered a UV-Visible spectrophotometer(UV-1800) to measure the absorption and transmission spectra of the RhB dye over a wavelength range of 190-1100 nm.

### Z-Scan technique

The Z-Scan measurements were split into two sections: a closed aperture and open aperture. Each component was powered by a continuous wave (CW) diode pump solid state blue laser with a wavelength of 457 nm and a power of 112 mW. The nonlinear refractive index was measured using a closed-aperture Z-Scan, while the nonlinear absorption coefficient was measured using an open-aperture Z-Scan. The beam was focused using a convex lens ( $f = 15$  cm), and the beam waist was measured at (0.025) cm at the

focus. The focus point's laser intensity was  $(20.408 \times 10^3)$  mW/cm<sup>2</sup>, and the sample was moved along the -axis. As a function of sample position, the transmittance through the sample was recorded.

## Results and discussion

In reaction to pH, the charge of RhB can shift from a zwitterion to a cation. Due to the change from the zwitterion to the cationic form of the dye, a progressive shift in the absorption spectra to lower energies (red shift) and an increase of the absorptivity (hyperchromic shift) is observed as the pH is dropped (pH=1)., However, as the pH rises (pH=10), the zwitterion form causes a progressive shift in the absorption spectra to higher energies (blue shift) and a decrease in absorptivity (hypochromic shift). The absorption spectra for concentrations ( $10^{-5}$ ) M of RhB dye were measured using a UV-Visible spectrophotometer before and after addition. The spectra in Fig.2 shows two bands, one in the UV region called the B-band at about (300-350) nm, which is attributed to electron transitions from the highest occupied molecular orbital (HOMO)  $a_{2u}$  to the lowest unoccupied molecular orbital (LUMO) eg. The second band is the Q-band, which occurs in the visible region at wavelengths between 520-580 nm and is caused by electron transitions from the (HOMO) to (LUMO). The electronic transition from  $\pi$  to  $\pi^*$  is related to the high-energy peak in the Q-band. Adding bases causes a drop in absorbance, while adding acids results in an increase in absorbance, linear absorbance index, refractive index, and transmittance, as well as a decrease in transmittance. This is consistent with Beer- Lambert law [15,16].

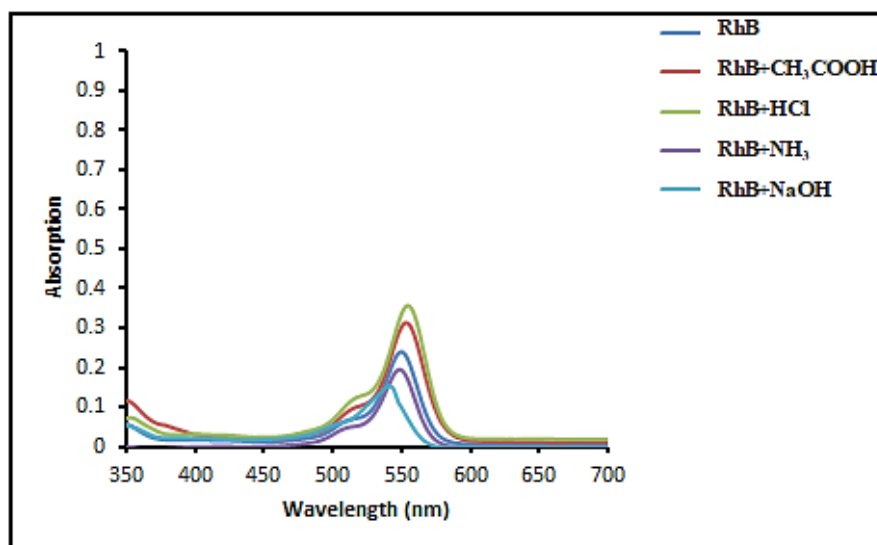


**Fig.2 : Absorption spectra of two molecular forms of RhB dye solution at concentration ( $10^{-5}$  M).**

The investigated nonlinear absorption coefficient. The results reveal that the open-aperture Z-Scan technique was used to quantify two molecular forms of the RhB dye solution at concentrations of ( $10^{-5}$ ) M in the methanol solvent. Fig.3 shows an open-aperture Z-Scan of samples in solvent at 457nm and 112 mW. This is a well-known phenomenon(two photon absorption) [15].

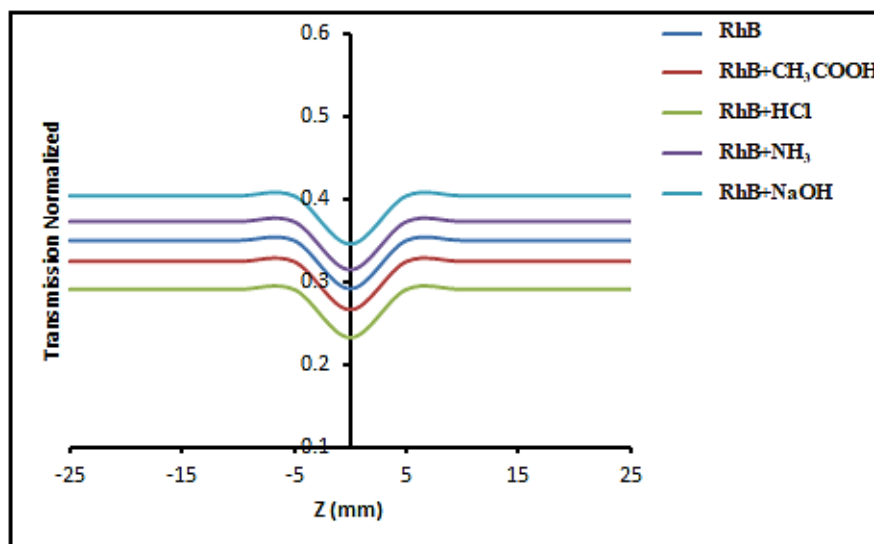


**Fig.3 : Open-aperture Z-Scan data of two molecular forms of RhB dye solution at concentration ( $10^{-5}$  M).**

At various distances from the a long way discipline of the pattern point, the transmittance conduct starts off evolved to act linearly (-Z). The transmittance curve begins offevolved declining withinside the close to discipline till it processes the minimal value (Tmin) on the pivot point (Z = zero mm). In the a long way discipline of the pattern position (+Z), the transmittance starts offevolved to increase a linear conduct. The two-photon absorption reasons the depth to extrade on this situation because the pattern passes via the middle of the beam. The variable transmittance values decided with the aid of using open aperture Z-scanning have been used to calculate the absorption coefficient [16].

The closed-aperture Z-Scan technique was used to measure the nonlinear refractive index of two molecular forms of RhB dye solution in the methanol solvent at a concentration of ( $10^{-5}$ ) M. Fig.4 shows the normalized transmittances of Z-Scan readings as a function of distance.

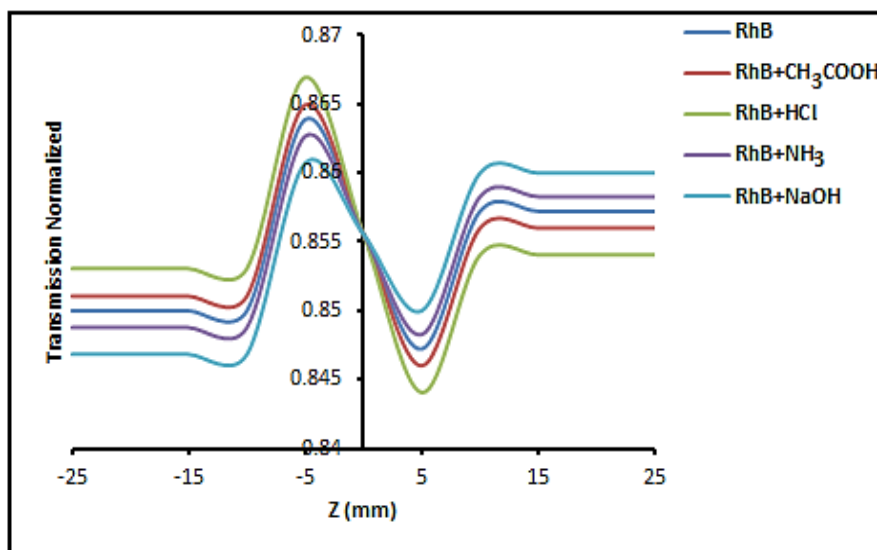


**Fig.4 : Closed-aperture Z-Scan data of two molecular forms of RhB dye solution at concentration ( $10^{-5}$  M).**

From (-15)to (15) mm, the nonlinear effect zone is expanded. The closed aperture Z-Scan data shows a transmittance peak followed by a valley curve, indicating that the refraction nonlinearity is negative ( $n_2 < 0$ ), resulting in the self-defocusing lensing in these samples [17].

To explain the Z-Scan behavior in the preceding pictures, the transmitted beam intensity is high and the transmittance remains relatively constant as the sample moves away from the focus. As the sample becomes closer to the beam focus, its intensity drops, causing self-lensing in the sample, which in turn causes the beam to collimate on the aperture in the far field, lowering the measured transmittance. Due to the self-lensing induced in the material by the intense laser beam, the fraction of light landing on the detector will fluctuate if the beam experiences any nonlinear phase shift as it travels through the focus region owing to the sample. As the sample is translated, the signal recorded by the detector will exhibit a peak and valley [18,19]. The difference in transmittance between the peak and valley can be used to calculate the size of the phase shift. The self-defocusing increases the beam divergence after the focal plane, resulting in a broadening of the beam at the focus and thus lowering the measured transmittance. Further from the focus ( $Z > 0$ ), nonlinear refraction is modest, leading to a Z-independent transmittance [20].

**Table1: The linear and nonlinear optical parameters of two molecular forms of RhB dye solution at concentration ( $10^{-5}$ ).**

Material	T	$\alpha_o$ [cm <sup>-1</sup> ]	$n_o$	$\Delta T_{P-V}$	$n_2 \times 10^{-11}$ [cm <sup>2</sup> /mW]	T(z)	$\beta \times 10^{-3}$ [cm/mW]
<b>RhB</b>	0.57	0.55	1.99	0.016	3.58	0.291	0.099
<b>RhB+CH<sub>3</sub>COOH</b>	0.48	0.72	2.21	0.018	4.11	0.266	0.091
<b>RhB+HCl</b>	0.44	0.82	2.34	0.022	4.99	0.232	0.080
<b>RhB+NH<sub>3</sub></b>	0.63	0.45	1.85	0.014	3.08	0.314	0.106
<b>RhB+NaOH</b>	0.69	0.36	1.72	0.010	2.28	0.345	0.116

We can see from this table that the values of nonlinear parameter for ( $n_2$ ) are decreased and ( $\beta$ ) increase with adding bases and increasing the values of linear parameters ( $n_o$  and  $\alpha_o$ ) with adding acids.

## 5. Conclusions

The cationic form has higher nonlinear indices of refraction than pure RhB dye, while pure RhB dye has a higher nonlinear index of refraction than the zwitterion form. Due to their diverse noncovalent interactions with distinct functional groups, systems are the crucial building blocks in supramolecular assembly. A notable example of this is applying  $\pi$ - $\pi$  interactions in supramolecular assembly.

The experimental statistics of the nonlinear optical responses of molecular varieties of RhB dye answer at concentrations ( $10^{-5}$ ) M confirmed that the pattern has self-defocusing phenomena and a terrible nonlinear refractive index, with a -photon absorption coefficient, which shows that the pattern may be utilized in nonlinear optical devices. In addition, the statistics we located approximately the crucial optical responses confirmed that we are able to use this laser dye in optical limiter applications.

## References

- [1] J. Zhang, Research on Experimental Accuracy of Laser Z-Scan Technology, AIP Conference Proceedings", 18, 2, (2017).
- [2] I. Hussein, A. Al-Saidi, S. Abdulkareem, Nonlinear Optical Properties and Optical Power Limiting



Effect of Giemsa dye, Optics and Laser Technology, 82, 150-156, (2016).

- [3] J. Karpiuk, Z. Grabowski and F. Schryver, Fluorescence Kinetics Study of Rhodamine B Lactone in Polar Aprotic Solvents - A global Analysis Approach, 104, 2, 133-142, (1992).
- [4] M. R. R. Vaziri, Z-Scan Theory for Nonlocal Nonlinear Media with Simultaneous Nonlinear Refraction and Nonlinear Absorption, Applied Optics, 52, 20, (2013).
- [5] Z. Fryad and S. Patil, Nonlinear Optical Properties and Optical Limiting Measurements of (1Z) (Dimethylamino) PhenylMethylene4-Nitrobenzocaroxy Hydrazone Monohydrate under CW Laser Regime, PhotonicsJournal, 4, pp. 182-188, (2014).
- [6] R.W. Boyd, Nonlinear Optics, 3<sup>rd</sup>, Academic Press, New York, (2008).
- [7] K. Abdali, F. Lamis, A. O. Abdmuslem, A. Abdulazeez, Enhancing some physics properties of cosmetic face powders, Journal of Global Pharma Rechnology, 10(5), pp. 75-78, (2018).
- [8] M.S. Bahae, A.A. Said, T. Wei, D.J. Hagan, QuantumElectron, E.W.V. Stryland, IEEE J, 26(3), pp. 760–769, (1990).
- [9] A. K. H. AL-Khalaf, K. Abdali, A. O. Mousa, M. A. Zghair, Preparation and structural Properties of Liquid crystalline materials and its transition metals complexes, Asian Journal of Chemistry, 31(2), pp. 393-395, (2019).
- [10] N. A. A. AL-Temeeme, S. K. Jameel, and A. A. Abd ALfahdawi, Photo-Physical Characterization of Rhodamine B in Liquid and Solid Solutions, Atti Della (Fondazione Giorgio Ronchi), (2007).
- [11] A. J. AL-Zuhairi, A. S. Allw, K. A. Obaid, S. R. Rasool, A. O. Mousa, Synthesis of Hyperbranched Polymers and Study of its Optical Properties, Journal of Engineering and Applied Sciences", 12, pp. 7800-7804, (2017).
- [12] A. H. Al-Hamdani, R. Nader, and R. Abdul Hadi, Spectral Properties of Rodamine B Dissolved in Chloroform, IOSR Journal of Research and Method in Education, 4(6), pp. 68-73, (2014).
- [13] I. L. Arbeloa, Solvent Effect on Photophysics on the Molecular forms of Rhodamine B, Chemical Physics Letters, 5(128), pp. 474-479, (1986).
- [14] Y. Saito, M. Kato, A. Nomura, and T. Kana, Simultaneous Three Primary Color Laser Emissions

From Dye Mixtures, *Appi. Phys. Lett.* 56(9), (1990).

[15] Noor. Al-Aaraji, A. O. Mousa, and B. A. Naser, Spectral and Linear Optical Characterization of Rhodamine B and Fluorescein Sodium Organic Laser Dyes Mixture Solutions, *Iraqi Journal of Science*", 60, pp. 69-74, (2019).

[16] R. Alnayli, Z. S. Shanon, and A. S. Hadi, " Study the Linear and Nonlinear Optical Properties for Laser Dye Rhodamine B", *Journal of Physics*, 1234, (2019).

[17] S. Sinha, A. Ray, and K. Dasgupta, Solvent Dependent Nonlinear Refraction in Organic Dye Solution, *Journal of Applied Physics*, 87,7, 3222-3225, (2000).

[18] F. Hajiesmaeilbaigi, A. Motamedi, Y. Golian, and E. B. Nik, Linear and Nonlinear Optical Properties of Rhodamine B Dye Solution with Au Nanoparticles, *Quantum and Nonlinear Optics II*, 8554, (2013).

[19] N. K. M. N. Srinivas, S. V. Rao, and D. N. Rao, Saturable and Reverse Saturable Absorption of Rhodamine B in Methanol and Water, *Optical Society of America*, 20(12), (2003).

[20] S. V. Rao, N. K. Srinivas, D. N. Rao, Nonlinear Absorption and Excited State Dynamics in Rhodamine B Studied Using Z-Scan and Degenerate Four Wave Mixing Techniques, 361, 439-445, (2002).

[21] JALIL, A. T., DILFY, S. H., KAREVSKIY, A., & NAJAH, N. (2020). Viral Hepatitis in Dhi-Qar Province: Demographics and Hematological Characteristics of Patients. *International Journal of Pharmaceutical Research*, 12(1). <https://doi.org/10.31838/ijpr/2020.12.01.326>

[22] Dilfy, S. H., Hanawi, M. J., Al-bideri, A. W., & Jalil, A. T. (2020). Determination of Chemical Composition of Cultivated Mushrooms in Iraq with Spectrophotometrically and High Performance Liquid Chromatographic. *Journal of Green Engineering*, 10, 6200-6216.

[23] Jalil, A. T., Al-Khafaji, A. H. D., Karevskiy, A., Dilfy, S. H., & Hanan, Z. K. (2021). Polymerase chain reaction technique for molecular detection of HPV16 infections among women with cervical cancer in Dhi-Qar Province. *Materials Today: Proceedings*. <https://doi.org/10.1016/j.matpr.2021.05.211>

- [24] Jalil, A. T., Kadhum, W. R., Khan, M. U. F., Karevskiy, A., Hanan, Z. K., Suksatan, W., ... & Abdullah, M. M. (2021). Cancer stages and demographical study of HPV16 in gene L2 isolated from cervical cancer in Dhi-Qar province, Iraq. *Applied Nanoscience*, 1-7. <https://doi.org/10.1007/s13204-021-01947-9>
- [25] Widjaja, G., Jalil, A. T., Rahman, H. S., Abdelbasset, W. K., Bokov, D. O., Suksatan, W., ... & Ahmadi, M. (2021). Humoral Immune mechanisms involved in protective and pathological immunity during COVID-19. *Human Immunology*. <https://doi.org/10.1016/j.humimm.2021.06.011>
- [26] Moghadasi, S., Elveny, M., Rahman, H. S., Suksatan, W., Jalil, A. T., Abdelbasset, W. K., ... & Jarahian, M. (2021). A paradigm shift in cell-free approach: the emerging role of MSCs-derived exosomes in regenerative medicine. *Journal of Translational Medicine*, 19(1), 1-21. <https://doi.org/10.1186/s12967-021-02980-6>
- [27] Hanan, Z. K., Saleh, M. B., Mezal, E. H., & Jalil, A. T. (2021). Detection of human genetic variation in VAC14 gene by ARMA-PCR technique and relation with typhoid fever infection in patients with gallbladder diseases in Thi-Qar province/Iraq. *Materials Today: Proceedings*. <https://doi.org/10.1016/j.matpr.2021.05.236>
- [28] Saleh, M. M., Jalil, A. T., Abdulkereem, R. A., & Suleiman, A. A. Evaluation of Immunoglobulins, CD4/CD8 T Lymphocyte Ratio and Interleukin-6 in COVID-19 Patients. *TURKISH JOURNAL OF IMMUNOLOGY*, 8(3), 129-134. <https://doi.org/10.25002/tji.2020.1347>
- [29] Turki Jalil, A., Hussain Dilfy, S., Oudah Meza, S., Aravindhana, S., M Kadhim, M., & M Aljeboree, A. (2021). CuO/ZrO<sub>2</sub> nanocomposites: facile synthesis, characterization and photocatalytic degradation of tetracycline antibiotic. *Journal of Nanostructures*.
- [30] Sarjito, Elveny, M., Jalil, A., Davarpanah, A., Alfakeer, M., Awadh Bahajjaj, A. & Ouladsmene, M. (2021). CFD-based simulation to reduce greenhouse gas emissions from industrial plants. *International Journal of Chemical Reactor Engineering*, (), 20210063. <https://doi.org/10.1515/ijcre-2021-0063>
- [31] Marofi, F., Rahman, H. S., Al-Obaidi, Z. M. J., Jalil, A. T., Abdelbasset, W. K., Suksatan, W., ... & Jarahian, M. (2021). Novel CAR T therapy is a ray of hope in the treatment of seriously ill AML patients. *Stem Cell Research & Therapy*, 12(1), 1-23. <https://doi.org/10.1186/s13287-021-02420-8>
- [32] Jalil, A. T., Shanshool, M. T., Dilfy, S. H., Saleh, M. M., & Suleiman, A. A. (2021). HEMATOLOGICAL AND SEROLOGICAL PARAMETERS FOR DETECTION OF COVID-

19. Journal of Microbiology, Biotechnology and Food Sciences, e4229.

<https://doi.org/10.15414/jmbfs.4229>

[33] Vakili-Samiani, S., Jalil, A. T., Abdelbasset, W. K., Yumashev, A. V., Karpisheh, V., Jalali, P., ... & Jadidi-Niaragh, F. (2021). Targeting Wee1 kinase as a therapeutic approach in Hematological Malignancies. DNA repair, 103203. <https://doi.org/10.1016/j.dnarep.2021.103203>

[34] NGAFWAN, N., RASYID, H., ABOOD, E. S., ABDELBASSET, W. K., AI-SHAWI, S. G., BOKOV, D., & JALIL, A. T. (2021). Study on novel fluorescent carbon nanomaterials in food analysis. Food Science and Technology. <https://doi.org/10.1590/fst.37821>

[35] Marofi, F., Abdul-Rasheed, O. F., Rahman, H. S., Budi, H. S., Jalil, A. T., Yumashev, A. V., ... & Jarahian, M. (2021). CAR-NK cell in cancer immunotherapy; A promising frontier. Cancer Science, 112(9), 3427. <https://doi.org/10.1111/cas.14993>

[36] Abosooda, M., Wajdy, J. M., Hussein, E. A., Jalil, A. T., Kadhim, M. M., Abdullah, M. M., ... & Almashhadani, H. A. (2021). Role of vitamin C in the protection of the gum and implants in the human body: theoretical and experimental studies. International Journal of Corrosion and Scale Inhibition, 10(3), 1213-1229. <https://dx.doi.org/10.17675/2305-6894-2021-10-3-22>

[37] Jumintono, J., Alkubaisy, S., Yáñez Silva, D., Singh, K., Turki Jalil, A., Mutia Syarifah, S., ... & Derkho, M. (2021). Effect of Cystamine on Sperm and Antioxidant Parameters of Ram Semen Stored at 4° C for 50 Hours. Archives of Razi Institute, 76(4), 923-931. <https://dx.doi.org/10.22092/ari.2021.355901.1735>

[38] Roomi, A. B., Widjaja, G., Savitri, D., Turki Jalil, A., Fakri Mustafa, Y., Thangavelu, L., ... & Aravindhan, S. (2021). SnO<sub>2</sub>: Au/Carbon Quantum Dots Nanocomposites: Synthesis, Characterization, and Antibacterial Activity. Journal of Nanostructures.

[39] Raya, I., Chupradit, S., Kadhim, M. M., Mahmoud, M. Z., Jalil, A. T., Surendar, A., ... & Bochvar, A. N. (2021). Role of Compositional Changes on Thermal, Magnetic and Mechanical Properties of Fe-PC-Based Amorphous Alloys. Chinese Physics B. <https://doi.org/10.1088/1674-1056/ac3655>

[40] Chupradit, S., Jalil, A. T., Enina, Y., Neganov, D. A., Alhassan, M. S., Aravindhan, S., & Davarpanah, A. (2021). Use of Organic and Copper-Based Nanoparticles on the Turbulator Installment in a Shell Tube Heat Exchanger: A CFD-Based Simulation Approach by Using Nanofluids. Journal of Nanomaterials. <https://doi.org/10.1155/2021/3250058>

[41] Raya, I., Chupradit, S., Mustafa, Y., H. Oudaha, K., M. Kadhim, M., Turki Jalil, A., J. Kadhim, A., Mahmudiono, T., Thangavelu, L. (2021). Carboxymethyl Chitosan Nano-Fibers for Controlled Releasing 5-Fluorouracil Anticancer Drug. Journal of Nanostructures,